MIMO CONTROL FOR AUTOMOTIVE COLDSTART

Pannag R. Sanketi [*,1] **J.Carlos Zavala** [*]
M.Wilcutts [*] **T.Kaga** [**] **J. K. Hedrick** [*]

[*] *Vehicle Dynamics and Control Laboratory, Etcheverry Hall, University of California, Berkeley, USA- 94720*
[**] *Toyota Technical Center U.S.A., Inc. Berkeley Laboratory, Tech. Research Dept.*

Abstract: The problem of controlling combustion engine emissions during the coldstart period is addressed by designing a MIMO sliding mode controller. The task of the controller is to track a given set of desired profiles of engine-out hydrocarbon emissions and catalyst temperature using spark timing and fuel injection rate as the inputs. This is an important step in solving the coldstart problem. The throttle is not used as a control input. Different profiles of desired engine-out hydrocarbons and catalyst temperatures are used to analyze the coldstart problem. Simulation results indicate that the controller tracks the desired profiles as long as the inputs are not saturated. The controller presented here could be used as a tool to investigate the optimal input profiles. Experiments are being carried out to validate the simulations. *Submitted to Fifth IFAC Symposium on Advances in Automotive Control*

Keywords: Coldstart, Model Based Control, MIMO Sliding control

1. INTRODUCTION

It is well known that during the coldstart period of a combustion engine, a large percentage of total cumulative hydrocarbon emissions are produced. Previous approaches to the problem can be broadly classified into two categories. One of them consists of changing the physical capabilities of the subsystems to reduce the emissions. For instance in (Nishizawa *et al.* 2000), new technologies are presented to achieve the SULEV (Super Ultra Low Emissions Vehicle) standards for an automotive engine: high velocity air and high swirl combustion, super low-heat mass substrate catalyst, two-stage high efficiency HC trap catalyst system and triple sensor highly accurate air-fuel ratio control system. In (Tanaka *et al.* 2001), a catalyst that reacts to the environment is presented. The second category considers the features of the plant as fixed and seeks strategies in which the control system can improve the emissions reduction performance of the engine. For instance, in (Fischer and Brereton 1997), the different strategies investigated to minimize HC emissions consist of finding optimal settings in the fuel injection pattern (single versus dual fuel injection pulse), the use of air-assisted fuel injection, and changes in the fuel injection mode (open intake valve injection versus closed intake valve injection). In (Arsie *et al.* 1998), models are developed to reduce the uncertainty in the prediction of emissions and improve the controller performance. Other efforts focus in reducing emissions by improving both aspects of the engine performance: changes in hardware and changes in control algorithms. In (Kaiser *et al.* 1998) and (Alkidas and Drews 1996),

[1] pannag@me.berkeley.edu

hydrocarbon emissions are compared with different setups for fuel preparation.

Coldstart controllers with various control inputs have been developed, though exhaust gas temperature, ignition timing and air-fuel ratio (AFR) continue to be used the most. Many of these try to optimize the trade-off between reducing the raw emissions and achieving a faster catalyst light-off. Refer to the following for related information (Aquino 1981),(Sun and Sivashankar 1998), (Souder and Hedrick 2004), (Tseng and Cheng 1999), (Shaw and Hedrick 2003) (Sanketi *et al.* 2005), (Baotic *et al.* 2003). (Tunestal *et al.* 1999) and (Lee *et al.* 2001) have used in-cylinder pressure measurement for control and estimation purposes. Hybrid automata have also been used in modeling and control, for example in (Sanketi *et al.* 2006) and (Giorgetti *et al.* 2005).

In this paper, it is assumed that the physical features of the engine components are fixed. We focus in designing controllers that track engine-out hydrocarbon emissions (HC_{raw}) and catalyst temperature (T_{cat}). The models for HC_{raw}, exhaust temperature (T_{exh}) and T_{cat} are presented in another paper submitted to this symposium.

The controller has a three-tier architecture: (i) Topmost is a T_{cat} dynamic surface controller that uses T_{exh} as the control input. (ii) At next level is a MIMO (2 output, 2 input) sliding mode controller that achieves desired profiles of T_{exh} and HC_{raw} using AFR and spark timing (Δ) as inputs. (iii) finally an AFR dynamic surface controller that uses the fuel injection rate ($\dot{m}_{fc}$) as the control input. See Fig. 1. First, different profiles of desired catalyst temperature and engine-out HC emissions based upon typical coldstart experimental data are tracked. Furthermore, the total tailpipe HC emissions in different cases and the feasibility of the control inputs are used as parameters to investigate the minimization of coldstart emissions.

2. CONTROLLER

2.1 Control Algorithm

The main idea in the control algorithm presented here is the combined use of the catalyst and the engine models. The inputs to the engine to reduce tailpipe emissions are determined using dynamic surface and MIMO sliding controllers. MIMO Sliding mode control laws are developed for T_{exh} and engine exhaust hydrocarbons HC_{raw}. Control laws are also developed for T_{cat} and the AFR. The control architecture is shown in the Figure 1.

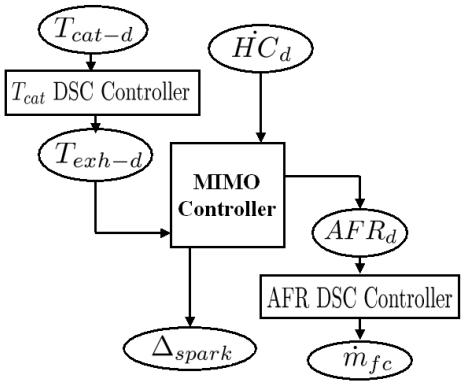

Fig. 1. The controller architecture

Overall strategy is driven by the T_{exh} and HC_{raw} models. Each of these, as described in (**?**), depends on both Δ and AFR. Together, these form a good platform for a MIMO control design. To start with, profiles of T_{cat} and HC_{raw} as given by typical coldstart experimental data are chosen as the desired profiles to be tracked. From the catalyst model, we know that T_{cat} depends mainly on T_{exh}. So we use the principle of dynamic surface controller, where T_{exh} is set such that the desired T_{cat} is achieved. Next in the hierarchy is a MIMO (2 inputs and 2 outputs) controller which uses the spark timing and the AFR to control the raw HC and T_{exh}. Then, the desired AFR is obtained through dynamic surface controller by using fuel injection rate as the input.

2.2 Catalyst Temperature Control

Catalyst temperature is mainly dependent on T_{exh}. Using dynamic surface control, we control T_{cat} treating T_{exh} as a synthetic input. We define a sliding surface equal to the difference between the actual and desired value of T_{cat}.

$$S_1 = T_{cat} - T_{cat,d} \tag{1}$$
$$\dot{S}_1 = \dot{T}_{cat} - \dot{T}_{cat,d}$$

Substitute for the dynamics of T_{cat} from (**?**). We get,

$$\dot{S}_1 = \frac{\dot{Q}_{gen} + \dot{Q}_{in} - \dot{Q}_{out} - \dot{Q}_{evap}}{mC_v + MC} - \dot{T}_{cat,d}$$

Treating T_{exh} as the input, design the control law to obtain

$$\dot{S}_1 = -\lambda_1 S_1$$

where λ_1 is a positive gain. This leads to

$$\bar{T}_{exh} = \frac{(\dot{T}_{cat,d} - \lambda_1 S_1)(mC_v + MC)}{\dot{m}_{exh} C_p} + \tag{2}$$
$$\frac{-\dot{Q}_{gen} + \dot{Q}_{out} + \dot{Q}_{evap} + \dot{m}_{exh} C_p T_{tp}}{\dot{m}_{exh} C_p}$$

where $\bar{T}_{exh}$ is the synthetic input. To track the desired value of the synthetic input, we need to find its derivative, which can lead to too many terms called the "explosion of terms" problem. Also, the term $\bar{T}_{exh}$ may include uncertainties which can lead to problems on differentiation. Hence, the desired value of T_{exh} to be tracked is found by passing the synthetic input through a low-pass filter so that explosion of terms and taking unknown derivatives is avoided. That is the basic principle of dynamic surface control.

$$\tau_T \dot{T}_{exh,d} + T_{exh,d} = \bar{T}_{exh} \tag{3}$$

Then, we use a MIMO sliding control design to achieve the desired profiles of exhaust gas temperature and raw HC using spark timing Δ and AFR as inputs.

2.3 MIMO control

We define a vector of sliding surfaces as follows:

$$\boldsymbol{S} = \begin{bmatrix} s_1 \\ s_2 \end{bmatrix} = \begin{bmatrix} T_{exh} - T_{exh,d} \\ HC_{raw} - HC_{raw,d} \end{bmatrix} \tag{4}$$

The $T_{exh,d}$ profile is obtained from the $T_{cat,d}$ as described in the previous subsection. Differentiating, and using the dynamics of T_{exh} and HC_{raw}, we set AFR and Δ to obtain

$$\dot{\boldsymbol{S}} = \begin{bmatrix} \dot{s}_1 \\ \dot{s}_2 \end{bmatrix} = -K\boldsymbol{S} \tag{5}$$

where, $K \in \mathbb{R}^{2x2}$, the gain on the MIMO control, is strictly a positive definite matrix. This will yield the desired profiles of AFR and Δ.

The outputs HC_{raw} and T_{exh} are coupled. These are two competing objectives playing an important role in the reduction of tailpipe emissions. It is important to choose a non-diagonal gain so that the coupling between the two outputs is not overlooked. If a diagonal matrix is chosen, it will be equivalent to two SISO sliding controllers.

2.4 AFR Control

To track the desired AFR, instead of defining a sliding surface on the AFR signal, it is more convenient to define a sliding surface on the fuel flow rate, as follows

$$S_2 = \dot{m}_{fo} - \dot{m}_{fo,d} \tag{6}$$

with

$$\dot{m}_{fo,d} = \frac{\dot{m}_{ao}}{AFR_d} \tag{7}$$

where AFR_d is the desired AFR and $\dot{m}_{ao}$ is the manifold out air flow rate. The commanded fuel flow is used as the input to obtain

$$\dot{S}_2 = -\lambda_2 S_2$$

where λ_1 is a positive gain. Using (6) and (8) together with the description of the fuel dynamics as given in (Sanketi *et al.* 2006), we get,

$$\epsilon\ddot{m}_{fc} + \frac{1}{\tau_f}\dot{m}_{fc} - \frac{1}{\tau_f}\dot{m}_{fo} - \ddot{m}_{fo,d} = -\lambda_2 S_2 \tag{8}$$

and expanding the term $\dot{m}_{fo,d}$ gives the equation for the control input

$$\ddot{m}_{fc} + \frac{1}{\epsilon\tau_f}\dot{m}_{fc} = \frac{1}{\epsilon\tau_f}\dot{m}_{fo} + \frac{1}{\epsilon}\left(\frac{\ddot{m}_{ao}}{AFR_d} + \frac{\dot{m}_{ao}}{AFR_d^2}A\dot{R}F_d\right) - \lambda_2 S_2 \tag{9}$$

As in the case of T_{cat} control, AFR_d is obtained by passing the synthetic input $A\bar{F}R$ through a low-pass filter so that explosion of terms and taking unknown derivatives is avoided.

$$\tau_{AFR}A\dot{F}R_d + AFR_d = A\bar{F}R_d \tag{10}$$

2.5 Notes on the controller

A nominal throttle profile during the coldstart is treated as an exogenous input to the system. Also, for the case of our analysis, the control input space was considered constant, whereas in practice it is dependent on the operating point.

The main sensors required for the controller implementation are the HC analyzer, a linear AFR sensor, exhaust and catalyst temperature sensors. Although, all the results presented in Section 3 are simulations, the inputs to the controller are based on experimental data.

Also, it is assumed that a full state feedback is available. Given HC and T_{exh} sensors, it is easy to implement the observers for the states. Currently, the possibility of estimating HC, AFR and T_{exh} using in-cylinder pressure measurements is being investigated.

Regarding the desired profiles, it should be noted that it is not verified if the profiles of $HC_{raw,d}$ and $T_{cat,d}$ used in this paper are the optimal ones for coldtart purposes. However, they provide a basis for analysis of optimality.

3. RESULTS AND DISCUSSION

Various sets of desired profiles of catalyst temperature ($T_{cat,d}$) and raw HC ($HC_{raw,d}$) are proposed to be tracked by the controller. The desired profiles cannot be chosen arbitrarily since there are physical constraints on the system. For example, T_{cat} will always have a plateau, because of the evaporation effect inside the catalyst. Similarly, the initial peak in the HC_{raw} cannot be completely wiped out because that will risk stalling

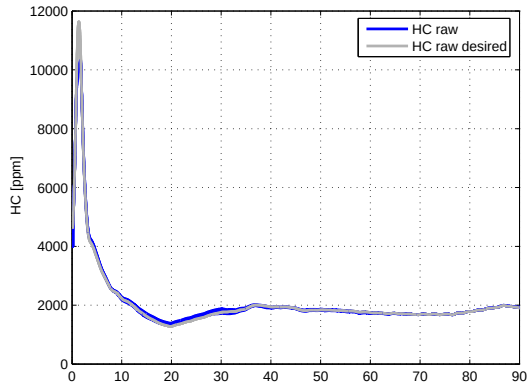

Fig. 2. HC_{raw} profiles (model and desired)- Run 1

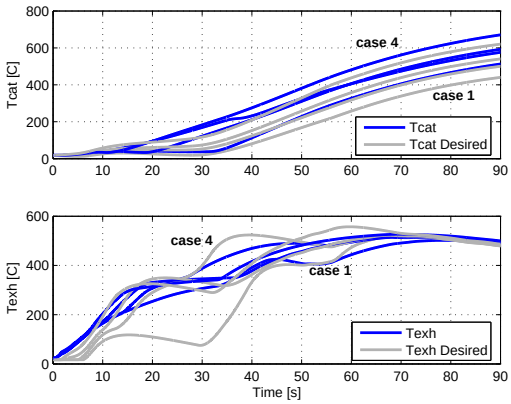

Fig. 3. T_{cat} and T_{exh} profiles (model and desired)- Run 1

the engine. Initially, those profiles were taken from experimental results of a typical coldstart run. The profiles were then modified to achieve a wider set of desired values. In this section, all the figures contain plots of a set of cases, which are grouped into runs. Where the plots show a single line, it means all the cases of the same run resulted in the same curve for that variable.

Figures 2 and 3 show the first set of desired profiles, $HC_{raw,d}$ and $T_{cat,d}$. $HC_{raw,d}$ desired was taken from a typical HC_{raw} coldstart profile. The corresponding $T_{cat,d}$ profile was offset by constants between -40C and 100C to obtain different $T_{cat,d}$ profiles. It should be noted that since the throttle position was treated as an exogenous input, the range of viable T_{cat} profiles was such that some of the $T_{cat,d}$ profiles could not be tracked. Note in Fig. 4 that the required $\dot{m}_{fc}$ was practically the same for different $T_{cat,d}$, however different profiles of Δ_{spark} were generated by the controller. The inputs show the expected trends. Different lightoff times (Fig. 6) meant different cumulative HC levels, as seen in Fig. 5.

Simulations were also performed using different $HC_{raw,d}$ profiles. In this case, the profiles were

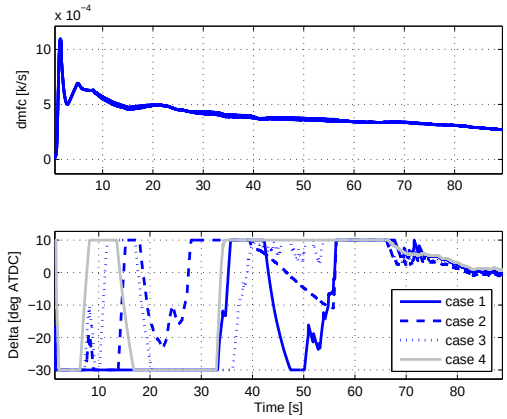

Fig. 4. Fuel injection rate and Spark timing - Run 1

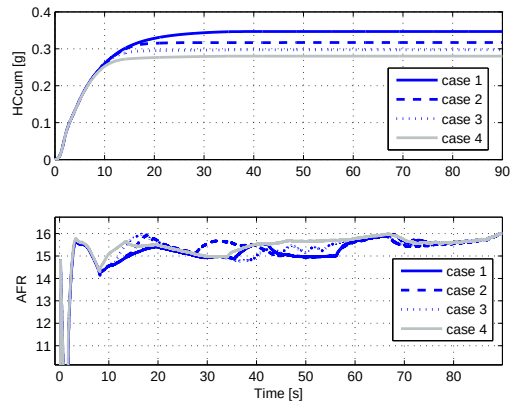

Fig. 5. Cumulative tailpipe HC and AFR- Run 1

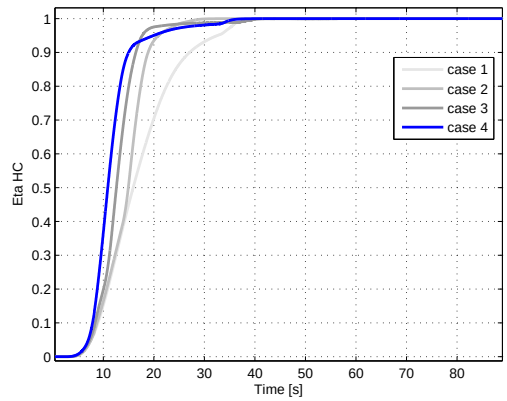

Fig. 6. Catalyst conversion efficiency- Run 1

obtained by multiplying a typical actual HC_{raw} coldstart profile by constants between 0.3 and 2.0. Fig. 8 shows $HC_{raw,d}$ together with the values of HC_{raw} given by the model. One of the desired profiles could not be tracked. The reason can be explained by the AFR profile in Fig. 11. The corresponding AFR_d reached the value of 16, which is the saturation level of AFR that we have used for the simulations.

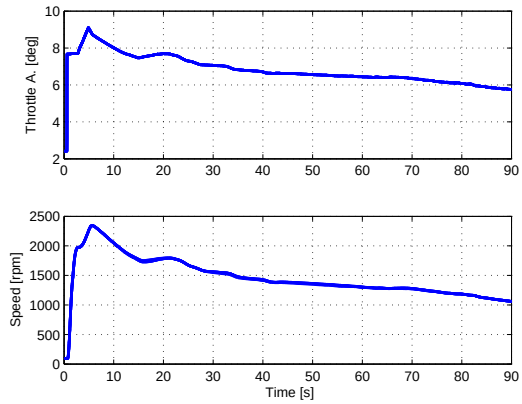

Fig. 7. Throttle angle and engine RPM- Run 1

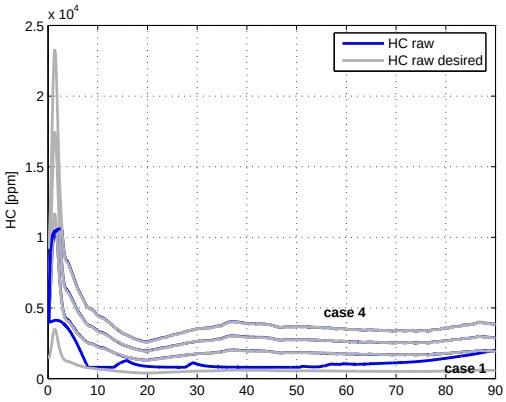

Fig. 8. HC_{raw} profiles (model and desired)- Run 2

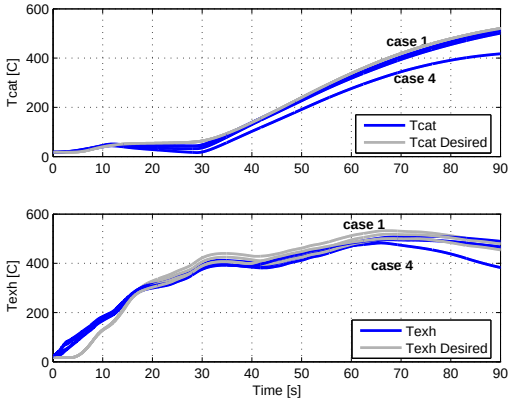

Fig. 9. T_{cat} and T_{exh} profiles (model and desired)- Run 2

Note in Fig. 11 the different levels of cumulative HC_{raw} reached by different simulations. Three of them are almost constant after 30s, however one of them still increases till about 60s. The catalyst efficiency shown in Fig. 12 explains this behavior , where one of the curves of efficiency drops below 50% between 30s and 60s. Further, a combination of different profiles of $T_{cat,d}$ and $HC_{raw,d}$ was simulated. The results for T_{cat} and HC_{raw} are shown in Fig. 13. The fuel injection rate, spark

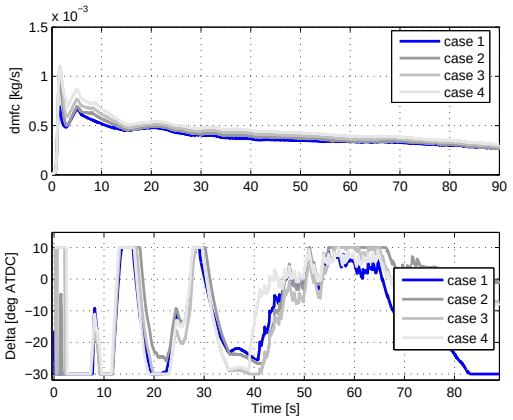

Fig. 10. Fuel injection rate and Spark timing - Run 2

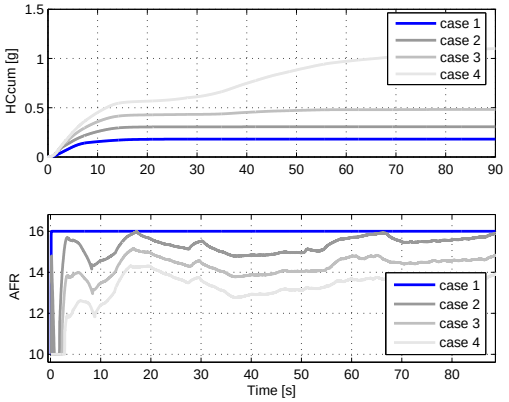

Fig. 11. Cumulative tailpipe HC and AFR- Run 2

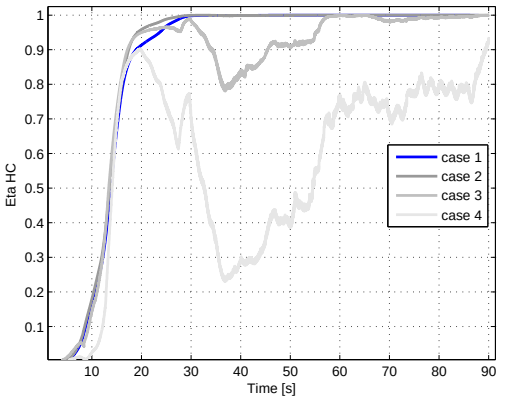

Fig. 12. Catalyst conversion efficiency- Run 2

timing, cumulative tailpipe HC and AFR are shown in Figures 14 and 15. Observe that the $HC_{raw,d}$ profiles can be tracked well, however one of the T_{cat} profiles cannot be tracked properly. This is due to the nature of the desired profiles and the value of the exogenous input. A higher HC_{raw} needs the AFR to be maintained rich and a retarded spark. Under such a scenario, T_{cat} cannot be maintained as low as you want. This basically illustrates the trade-off during coldstart. Also note

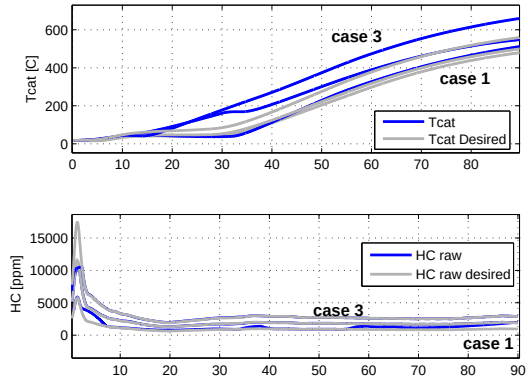

Fig. 13. Catalyst temperature and HC emissions (model and desired)- Run 3

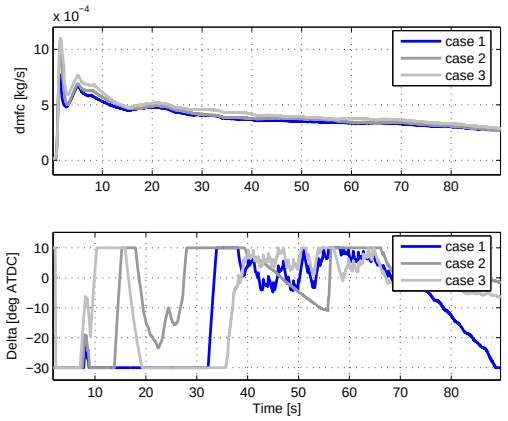

Fig. 14. Fuel injection rate and Spark timing - Run 3

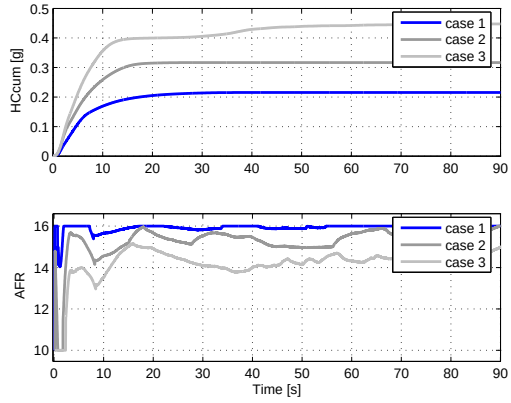

Fig. 15. Cumulative tailpipe HC and AFR- Run 3

that even though the catalyst conversion efficiency η_c (shown in Fig. 16) for case 1 reaches 1 at around 30s, the total cumulative HC are less than for that case 3, where η_c reaches 1 in about 15s. The reason is the difference in HC_{raw} emissions level.

Simulations were also performed with different throttle angle profiles, as shown in Fig. 17. The profiles were obtained by multiplying three different factors (0.7, 1.0 and 1.3) to a typical cold-

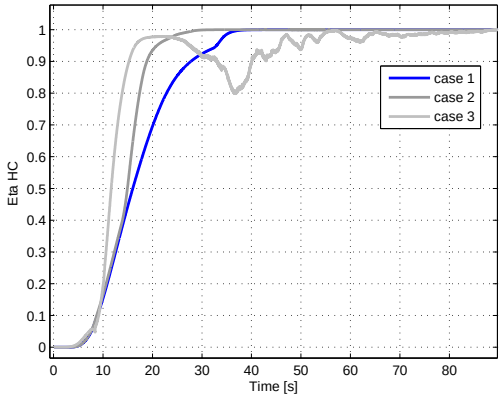

Fig. 16. Catalyst conversion efficiency- Run 3

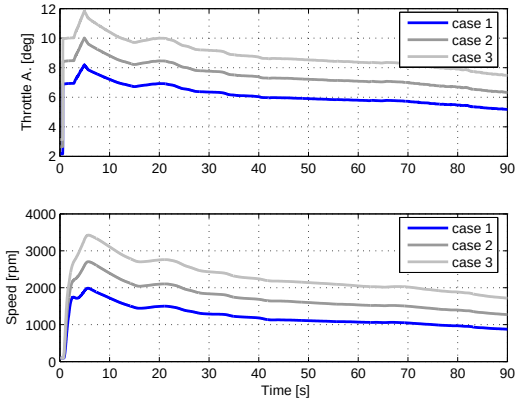

Fig. 17. Throttle angle profiles and engine speeds - Run 4

start throttle angle profile given by the ECU. The desired T_{cat} was chosen to be the same for the different throttle angles. As seen in Figures 18 and See Fig. 20, the system could not track the desired profile for one of the cases, viz. case 1. At low engine speed, the engine pressure is low due to which the combustion quality is low. Hence, HC_{raw} cannot be maintained as low as desired and T_{cat} cannot be increased as fast as desired. The low T_{cat} affects adversely η_c, as seen in Fig. 19.

In another set of experiments (Run 5), different constant profiles for the accessory torque were used as disturbances during the system simulations. The values of the accessory torque were between 10 and 70 N-m The throttle and engine speeds are shown in Fig. 21. The desired T_{cat} and T_{exh} were the same for all different cases of the simulation. However in one of them the desired profiles could not be achieved, mainly due to the low values of crankshaft speed for that case. See Fig. 22 The degradation in the HC_{tp} emissions can be observed in Fig. 23 and Fig. 24. The performance in case 3 is related to the low values of η_c. This case has the largest accessory torque (70 N-m).

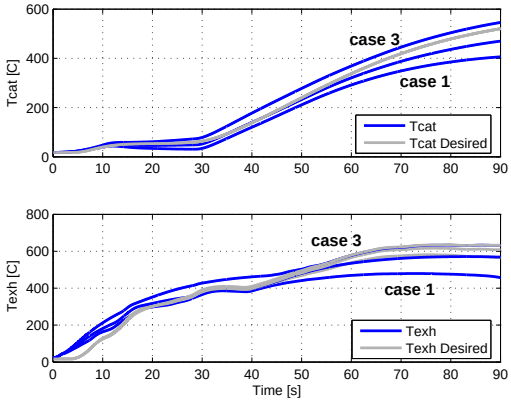

Fig. 18. Catalyst and exhaust temperature profiles (model and desired)- Run 4

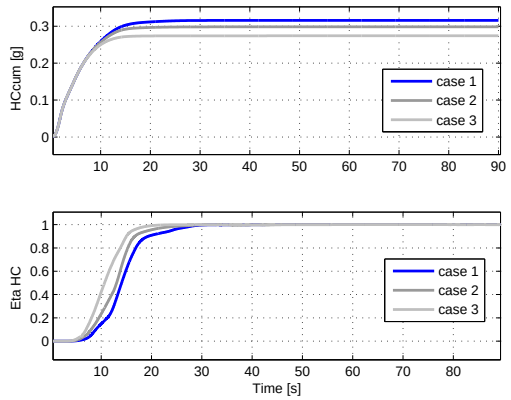

Fig. 19. Cumulative HC emissions and Catalyst conversion efficiency- Run 4

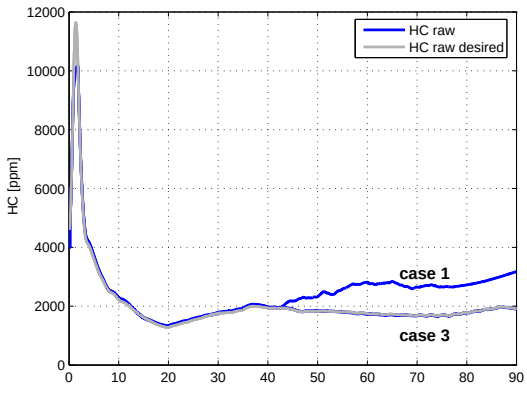

Fig. 20. $HC_{raw,d}$ and HC_{raw} (model and desired)- Run 4

4. CONCLUSIONS

A coldstart controller with three components was designed. The first component is a DSC (dynamic surface control) controller which tracks a desired T_{cat} profile . The second is a MIMO (multiple input-multiple output) sliding mode controller that tracks HC_{raw} and T_{exh}. The third one is a

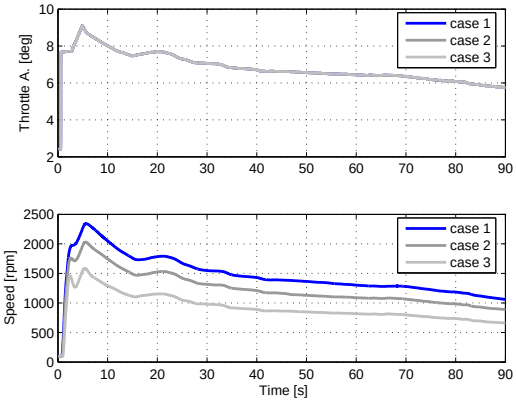

Fig. 21. Throttle angle profiles and engine speeds - Run 5

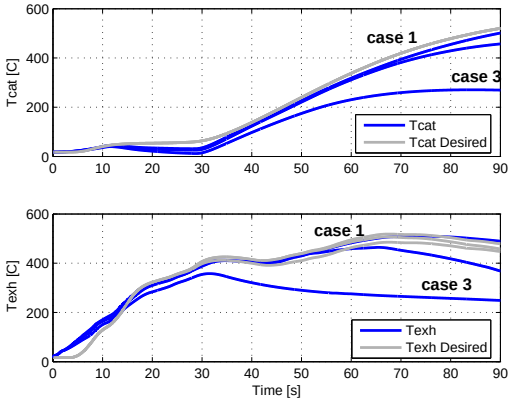

Fig. 22. Catalyst and exhaust temperature profiles (model and desired)- Run 5

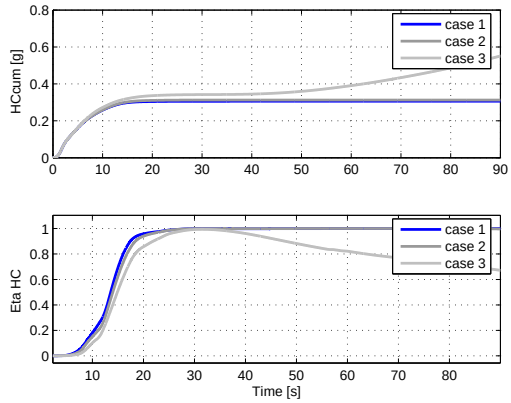

Fig. 23. Cumulative HC emissions and Catalyst conversion efficiency- Run 5

DSC AFR controller. Simulations are performed using typical coldstart HC_{raw} and T_{cat} profiles as initial tracking references for the controller. The desired HC_{raw} and T_{cat} were modified from their respective initial profiles and the changes in tailpipe emissions (HC_{tp}) were analyzed. The tradeoff of fast light-off vs. low HC_{tp} was evident when several combinations of desired HC_{raw}

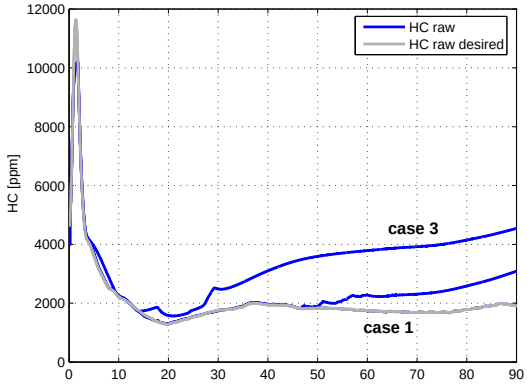

Fig. 24. $HC_{raw,d}$ and HC_{raw} (model and desired)- Run 5

profiles with desired T_{cat} were used. Simulations with external disturbances in the throttle angle and accessory torque showed some degradation in the performance of the controller. In all the cases, changes in the desired HC_{raw} seemed to have a larger effect on tailpipe emissions than the changes in the desired T_{cat}.

At this time, experiments are being carried out to validate the results of simulations. Also, methods are being analyzed to approach the problem of the optimization of the system. The use of the actual allowed ranges of control inputs represent an aspect of the optimization problem, too. In practice, the control input space is dependent on the operating point. For the case of our simulations, for ease of analysis, it was considered constant. The controller was designed based on the engine model presented in another paper submitted to this symposium.

5. ACKNOWLEDGEMENTS

Authors acknowledge the financial support provided by CONACYT (Consejo Nacional de Ciencia y Tecnología de Mexico) and by the Center for Hybrid and Embedded Software Systems (CHESS) at UC Berkeley, which receives support from the National Science Foundation (NSF award #CCR-0225610), the State of California Micro Program, and the following companies: Agilent, Bosch, DGIST, General Motors, Hewlett Packard, Infineon, Microsoft, National Instruments, and Toyota.

REFERENCES

Alkidas, A.C. and R.J. Drews (1996). Effects of mixture preparation on hc emissions of a s.i. engine operating under steady-state cold conditions. *SAE Technical Paper 961958*.

Aquino, C.F. (1981). Transient a/f control characteristics of the 5 liter central fuel injection engine. *SAE 810494*.

Arsie, I., C. Pianese and G. Rizzo (1998). Models for the prediction of performance and emissions in a spark ignition engine - a sequentially structured approach. *SAE Technical Paper 980779*.

Baotic, M., M. Vasak, M. Morari and Nedjeljko Peric (2003). Hybrid systems theory based optimal control of an electronic throttle. *Proceedings of the American Control Conference* pp. 5209–5214.

Fischer, H.C. and G.J. Brereton (1997). Fuel injection strategies to minimize cold-start hc emissions. *SAE Technical Paper 970040*.

Giorgetti, N., A. Bemporad, I. Kolmanovsky and D. Hrovat (2005). Explicit hybrid optimal control of direct injection stratified charge engines.

Kaiser, E., W.O. Siegl, P. Lawson, F.T. Conolly, C.F. Cramer, K.L. Dobbins, P.W. Roth and M. Smokovitz (1998). Effect of fuel preparation on cold-start hydrocarbon emissions from a spark-ignite engine. *SAE Technical Paper 961957*.

Lee, A.T., M. Wilcutts, P. Tunestal and J.K.Hedrick (2001). A method of lean air-fuel ratio control using combustion pressure measurement. *Society of Automotive Engineers of Japan, Inc. and Elsevier Science* pp. 389–393.

Nishizawa, K., S. Momoshima and M. Koga (2000). Nissan's gasoline sulev technology. *SAE Technical Paper 2000-01-1583*.

Sanketi, P.R., J. Carlos Zavala and J. K. Hedrick (2005). Dynamic surface control of engine exhaust hydrocarbons and catalyst temperature for reduced coldstart emissions. In: *Proc. of International Federation of Automatic Control (IFAC) Conference*. Prague, Czech Rep.

Sanketi, P.R., J.C. Zavala and J.K. Hedrick (2006). Automotive engine hybrid modeling and control for reduction of hydrocarbon emissions. *International Journal of Control* **79**(5), 449–464.

Shaw, B. and J. K. Hedrick (2003). Closed-loop engine coldstart control to reduce hydrocarbon emissions. *Proceedings of the American Control Conference* pp. 1392–1397.

Souder, J. and J. K. Hedrick (2004). Adaptive sliding mode control of air-fuel ratio in internal combustion engines. *International Journal of Robust and Nonlinear Control* **14**(6), 525–541.

Sun, J. and N. Sivashankar (1998). Issues in cold start emission control for automotive ic engines. *Proceedings of the American Control Conference* pp. 1372–1376.

Tanaka, H., M. Uenishi and I. Tan (2001). An intelligent catalyst. *SAE Technical Paper 2001-01-1301*.

Tseng, T.C. and W.K. Cheng (1999). An adaptive air/fuel ratio controller for si engine throttle transients. *SAE 1999-01-0552*.

Tunestal, P., M. Wilcutts, A.T. Lee and J.K. Hedrick (1999). In-cylinder measurement for engine cold-start control. *Proceedings of the 1999 IEEE International Conference on Control Applications* pp. 460–464.